

See discussions, stats, and author profiles for this publication at: <https://www.researchgate.net/publication/51244089>

# Conducting Polyaniline Nanoparticles and Their Dispersion for Waterborne Corrosion Protection Coatings

ARTICLE in ACS APPLIED MATERIALS & INTERFACES · JUNE 2011

Impact Factor: 6.72 · DOI: 10.1021/am200488m · Source: PubMed

---

CITATIONS

40

---

READS

52

## 2 AUTHORS:



Fei Chen

Boston University

13 PUBLICATIONS 122 CITATIONS

SEE PROFILE



Peng Liu

Lanzhou University

242 PUBLICATIONS 3,924 CITATIONS

SEE PROFILE

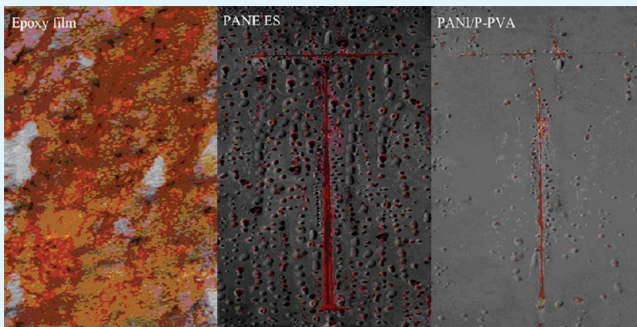
# Conducting Polyaniline Nanoparticles and Their Dispersion for Waterborne Corrosion Protection Coatings

Fei Chen and Peng Liu\*

Key Laboratory of Nonferrous Metal Chemistry and Resources Utilization of Gansu Province and Institute of Polymer Science and Engineering, Lanzhou University, Lanzhou 730000, China

**ABSTRACT:** A novel approach for preparing waterborne corrosion protection polyaniline (PANI)-containing coatings was developed. First, conducting polyaniline/partially phosphorylated poly(vinyl alcohol) (PANI/P-PVA) spherical nanoparticles with significant dispersibility in aqueous media were prepared by the chemical oxidative dispersion polymerization in presence of partially phosphorylated poly(vinyl alcohol) (P-PVA). The PANI/P-PVA-containing coatings with different PANI/P-PVA contents were then prepared, employing waterborne epoxy resin as the matrix. The corrosion protection property of PANI/P-PVA-containing coatings on mild steel was investigated by salt spray test and electrochemical impedance spectroscopy (EIS) technique in 3.0 wt % NaCl aqueous solution. The results indicated that the waterborne PANI/P-PVA-containing coatings (PANI/P-PVA content, 2.5 wt %) could offer high protection because the impedance values remained at higher than  $1 \times 10^7 \Omega \text{ cm}^2$  after 30 days of salt spray tests. All the results were compared with these of the waterborne coatings containing PANI nanoparticles in the emeraldine salt form (PANI ES), and the protection mechanism was also proposed with the evidence of scanning electron microscope (SEM) and X-ray photoelectron spectrometry (XPS).

**KEYWORDS:** polyaniline, waterborne coatings, steel, corrosion protection, electrochemical impedance spectroscopy



## INTRODUCTION

Among the conducting polymers, polyaniline (PANI) is found to be one of the most promising materials because of ease of synthesis, high electrical conductivity, nontoxic property, good environmental and chemical stability, chemical redox reversibility, and low cost.<sup>1,2</sup> Many works indicated that PANI is a good candidate for anticorrosion coatings on steel in acid and saline media.<sup>3–6</sup> The mechanism of corrosion protection of steel by PANI coatings has also been studied, and a number of operating mechanisms were reported such as anodic protection, barrier protection, corrosion inhibitors, shift of electrochemical interface, etc.<sup>7–10</sup>

The anodic protection is evidenced by the widely observed shift in corrosion potential into the passive region, although there is a large variation in the magnitude of the shift observed in different investigations.<sup>11</sup> Wessling et al. claimed that the corrosion protection of PANI on steel was attributed to an increase in the corrosion potential and to the passive oxide layer between PANI coatings and the steel surface.<sup>12</sup> The passive oxide layer was confirmed by scanning electron microscopy (SEM), X-ray photoelectron spectrometry (XPS), and Raman spectroscopy techniques. The passive oxide layer, mainly composed of  $\text{Fe}_2\text{O}_3$  above a very thin  $\text{Fe}_3\text{O}_4$  layer, was believed to be a result of the electrochemical reaction between polymer and Fe surface.<sup>12,13</sup> Beard and Spellane argued that PANI in oxidation state could catalyze or otherwise enable passivation of steel surfaces, through electrochemical interaction with steel substrate.<sup>14</sup> They found that the cold rolled steel/PANI sample, dried at high temperature

in air, produced a thin film of PANI in an oxidation state higher than the PANI film applied to the steel. When heating a glass/PANI sample in air the same oxidation effect was not found, suggesting the need for an electrochemical partner, or thermal conductor, to facilitate the migration of charge. Kinlen et al also indicated the passivation of steel surface through the steel anodization by PANI and the formation of an insoluble iron-dopant salt at the metal surface.<sup>15</sup> Torresi et al. held that PANI acted as anion storage, which could release anions when breakage occurs to the coatings, and it was suggested to form a second physical barrier that counteracts penetration of aggressive ions.<sup>16</sup> In general, PANI exhibits redox conversion and provides corrosion protection in PANI-containing coatings, but the effect also depends on the metal substrates and the coating formulations.

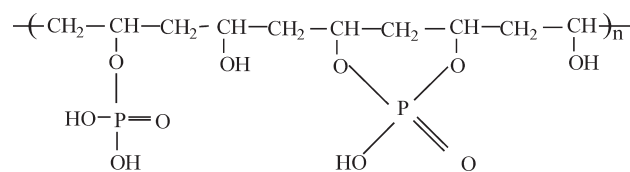
In recent years, environmental considerations make the research on anticorrosion coatings shift from solvent-based system to water-based system.<sup>17,18</sup> PANI dispersions have also been utilized to prepare the waterborne anticorrosion coatings in a form of dispersion.<sup>19</sup> However, this kind of waterborne coating is not very effective on the corrosion protection of steel because of its poor dispersibility and exceeding volume fraction (>15 vol%) of PANI dispersions. PANI has a poor adhesion and, moreover, during the redox processes changes its density, and thus also its volume. The macroscopic PANI particles and their high volume

**Received:** April 18, 2011

**Accepted:** June 23, 2011

**Published:** June 23, 2011

Scheme 1. Simplified Structure of the P-PVA



fraction are likely to damage the mechanical properties of coatings and increase the permeability to small molecules. To get a waterborne corrosion protection coating with high performance, it is necessary to improve the dispersibility of PANI in aqueous media.<sup>20</sup> Polymerization of aniline in the presence of water-soluble polymeric stabilizers (e.g., poly(*N*-vinyl pyrrolidone), poly(methyl vinyl ether), and poly(vinyl alcohol) (PVA))<sup>21</sup> is a well-known technique to improve the solubility of PANI. However, these stabilizers might impair PANI anticorrosion ability because of the presence of hydrophilic groups.

Partially phosphorylated poly(vinyl alcohol) (P-PVA) is a phosphoric ester by phosphorylation of PVA with phosphoric acid.<sup>22</sup> P-PVA exhibits more effective stabilization in polymerization, higher water resistance and mechanical property than PVA and could be used as metal complexes, ionic conducting polymer materials, anionic polyelectrolyte hydrogels, and polymeric stabilizer.<sup>23</sup> Additionally, phosphate compounds can be used as corrosion inhibitors for steel,<sup>24</sup> and PANI with phosphate dopant is very effective in corrosion protection.<sup>25,26</sup> Sathiyarayanan et al. synthesized a phosphate-doped PANI and a solvent-based corrosion protection coating containing 1.0 wt % PANI with epoxy binder. The corrosion-resistant property of the phosphate-doped PANI-containing coatings on steel was found out by open circuit potential (OCP) and electrochemical impedance spectroscopy (EIS) in 0.1N HCl, 0.1N H<sub>3</sub>PO<sub>4</sub>, and 3.0 wt % NaCl for the duration of 50 days.<sup>27</sup> This coating is able to protect steel effectively in 0.1N H<sub>3</sub>PO<sub>4</sub> and 3.0 wt % NaCl media. But that phosphate doped PANI exhibits poor dispersibility and yields aggregation in aqueous media, indicating that it is not an appropriate candidate for waterborne corrosion protection coatings.

In this work, we directed our efforts on the investigation of possibility for creation of waterborne anticorrosion coatings on mild steel with aqueous epoxy resin as matrix based on recently developed polyaniline/partially phosphorylated poly(vinyl alcohol) (PANI/P-PVA) nanoparticles.<sup>28</sup> Partially phosphorylated poly(vinyl alcohol) (P-PVA) acted as the codopant and polymeric stabilizer in this system.

## EXPERIMENTAL SECTION

**Materials.** Aniline (99.9 wt %) and ammonium persulfate (APS, 99.9 wt %) were obtained from Aldrich chemicals. Poly(vinyl alcohol) (PVA), phosphoric acid (H<sub>3</sub>PO<sub>4</sub>, 85 wt %), and hydrochloric acid (HCl, 36–38 wt %) were supplied by Baiyin Chemical Agents Company, China. Waterborne epoxy resin (model BH-620) and polyamide hardener (Model No. BECKOPOX EH623W/80WA) were supplied by Black Horse Chemical Co., Ltd., China, and Cytec Industries Inc., respectively.

**Synthesis of the PANI/P-PVA Nanoparticles.** P-PVA was prepared by phosphorylation of PVA with phosphoric acid in an aqueous media according to the literature.<sup>29</sup> The degree of substitution and molar ratio of monoester to diester of the P-PVA are 17.8 mol % and 2.2:1,

respectively. The simplified structure of P-PVA is illustrated in Scheme 1. PANI/P-PVA nanoparticles were synthesized through a procedure presented in our previous work.<sup>28</sup> Two grams of aniline was well-mixed with 300 mL of 0.2 M HCl aqueous solution containing 1.0 g of P-PVA. The system was cooled at 0 °C followed by the addition of 50 mL of 0.2 M HCl aqueous solution of APS; the mole ratio of aniline to APS was 2:1. The polymerization was allowed to proceed for 24 h while maintaining the temperature between ±2 °C. A dark-green colloidal PANI/P-PVA dispersion could be obtained. Then, PANI/P-PVA nanoparticles were isolated by centrifugation and washed repeatedly with distilled water. For comparison, the conventional PANI ES was prepared under the similar condition in absent of the P-PVA.

**Characterization of the PANI/P-PVA Nanoparticles.** Images of the PANI/P-PVA nanoparticles were obtained using transmission electron microscopy (TEM) on a JEOL JEM-1200EX/S transmission electron microscope. The structure of the PANI/P-PVA nanoparticles was characterized by Fourier transform infrared spectra (FTIR) (Impact 400, Nicolet, Waltham, MA) and X-ray diffraction (XRD) (Rigaku D/MAX 2000 diffractometer) following standard routines. The PANI/P-PVA powder was compressed into a disk pellet of 10 mm in diameter with a hydraulic pressure at 30 MPa, and the electrical conductivity of the PANI/P-PVA nanoparticles was measured using SDY-4 four-probe meter at room temperature.

**Preparation of Waterborne PANI/P-PVA Containing Coatings.** PANI/P-PVA nanoparticles were redispersed in distilled water in an ultrasonic bath for 3 h. Then, the PANI/P-PVA redispersion and the waterborne epoxy resin emulsion (model BH-620) with epoxy equivalent weight 500–650 were mixed and stirred until a homogeneous dispersion was formed (~5 h). The PANI/P-PVA pigmented epoxy resin emulsion was cured with a polyamide hardener (Model No. BECKOPOX EH623W/80WA) with amine value 210–230 mg. Waterborne PANI/P-PVA-containing coatings with PANI/P-PVA content of 1.0 wt % (1.0 wt % PANI/P-PVA), 2.5 wt % (2.5 wt % PANI/P-PVA), and 4.0 wt % (4.0 wt % PANI/P-PVA) were prepared. Waterborne PANI ES-containing coating with PANI ES content of 2.5 wt % (2.5 wt % PANI ES) was also prepared for comparative studies. The prepared coatings were applied over sand blasted (SA2.5) mild steel panels by a dipping method and cured in a furnace at 80 °C for 2 h. Then, the panels were allowed to completely dry for 24 h at 40 °C. The thickness of the coatings was measured by a BYK-Gardner thickness meter (model 7500). The dry film thickness of all the samples was 90 ± 10 μm.

**Evaluation of Physical Properties.** The tensile strength test of coatings/films was carried out on a tensile tester (Model TY8000, Jiangdu Tianyuan Test Machine Co., Ltd., China) with a speed of 50 mm/min. All data were the average values of three runs. Impact resistance was measured according to ASTM G14–04 (Falling Weight Test). Pencil hardness measured according to ASTM D3363–00 by using a set of equivalent calibrated wood pencils meeting the scale of hardness from 6 B (softer) to 6 H (harder). The coated panel was placed on a firm horizontal surface. Adhesion strength was measured according to ASTM D3359–02 by cross-cut technique, the adhesion strength ranges from 0 to 5 B, and 5 B is the upper. The gas permeability for the coatings was determined by air transmission through the films according to ASTM standard E 96.<sup>30</sup> The water vapor permeation for membrane was measured according to the previous literature.<sup>31</sup> All resulting data were the average values of three runs, with all measuring relative errors within 5.0%.

**Salt Spray Tests.** Coated mild steel panels were prepared by coating on sand blasted (SA 2.5) specimen of size 15 cm × 10 cm × 0.1 cm. The coated panels were exposed to salt spray of 3.0 wt % NaCl solution as per ASTM B117 for 720 h.

**Electrochemical Measurements.** The electrochemical behavior of waterborne PANI/P-PVA-containing coatings on mild steel was



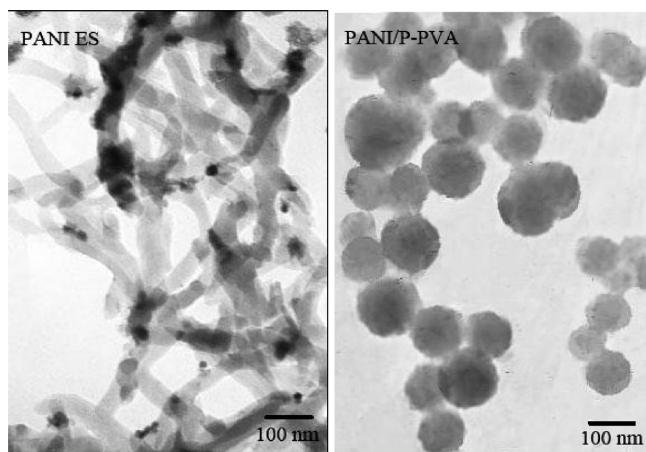


**Figure 1.** TEM images of PANI ES and PANI/P-PVA nanoparticles.

investigated in 3.0 wt % NaCl solution by different electrochemical measurements, using a three-electrode electrochemical cell with a saturated Ag/AgCl reference electrode and a Pt mesh as counter electrode. The coated steels were exposed to 3.0 wt % NaCl solution and the exposed area was 1.0 cm<sup>2</sup>. The OCP of the sample was recorded continuously with respect to SCE using a high input impedance voltmeter (HP 973 A), and then daily over a prolonged exposure period of up to 50 days. During the exposure, EIS measurement was performed once a day to monitor the change of coatings. EIS spectra were acquired at the OCP with a frequency range of 0.01 Hz to 100 kHz with an ac amplitude of 20 mV and analyzed by the electrochemical analyzer (supplied by CH instruments, USA). Higher amplitude of 20 mV is used since the impedance of the system is very high. From the impedance plots, the coatings resistance ( $R_c$ ) and the coatings capacitance ( $C_c$ ) values were calculated using an equivalent circuit.<sup>32</sup>

**Surface Characterization.** After 50 days exposure to 3.0 wt % NaCl, pure epoxy, 2.5 wt % PANI ES, and 2.5 wt % PANI/P-PVA coated steel samples were stripped of coatings mechanically. They were then ultrasonically degreased in acetone followed by degreasing with ethanol and finally washed thoroughly with distilled water. The samples were allowed to dry in vacuum chamber at 40 °C for 2 h and then cut to 3 mm × 5 mm dimension for surface characterization. The surface morphology of the interface between treated steel and coatings was examined using a JEOL SEM. For XPS analysis, a PH I-5702 spectrometer was employed with an unmonochromatized Al K $\alpha$  X-ray source. The binding energies are quoted relative to hydrocarbon C 1s at 284.6 eV. The preparation of the sample was completed little time before the measurement by XPS to minimize additional contamination.

## RESULTS AND DISCUSSION

**Characterizations of the PANI/P-PVA Nanoparticles.** TEM images (Figure 1) are used to view the morphology and size of the PANI ES and PANI/P-PVA nanoparticles. It was found that the PANI ES exhibited fibrillar morphology with large agglomerates. Although the PANI/P-PVA spherical particles had uniform diameters in 60–100 nm, and few agglomerates could be observed, P-PVA could act as an effective polymeric stabilizer for the PANI aqueous dispersions. The digital photos (Figure 2) show the dispersibility of the PANI ES and PANI/P-PVA nanoparticles in distilled water. For the PANI ES redispersion, the PANI precipitated completely after being stated for 1 day. In contrast, for the PANI/P-PVA nanoparticle redispersion, no

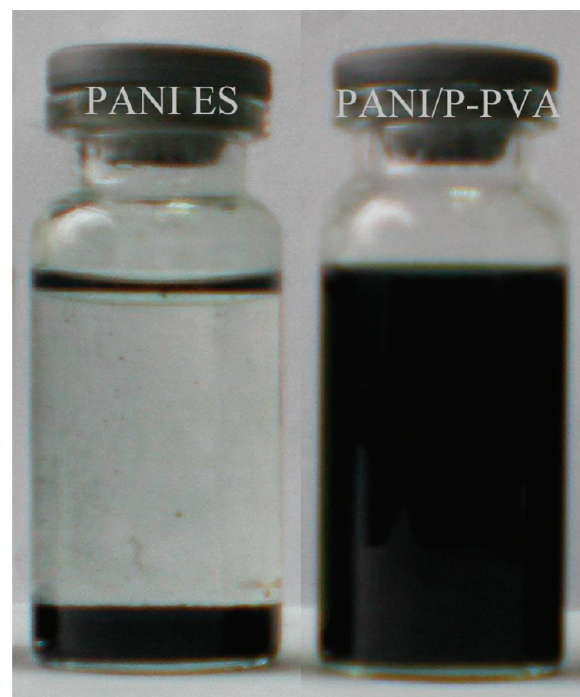


**Figure 2.** Dispersibility of PANI ES in aqueous media for 1 day, and PANI/P-PVA in aqueous media for 14 days.

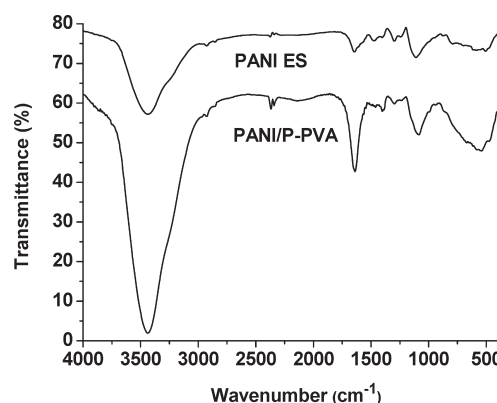


**Figure 3.** FTIR spectra of PANI ES and PANI/P-PVA.

precipitation was found after sedimentation for 14 days. The results indicated that the dispersibility of the PANI/P-PVA nanoparticles in aqueous media was excellent because of the effective stabilization of P-PVA. The excellent dispersibility of the PANI/P-PVA nanoparticles is conducive to getting waterborne PANI-containing coatings with dense and compact structure to slow down the diffusion of water as well as other ions into coatings.

The FTIR spectra of the PANI ES and PANI/P-PVA are presented in Figure 3. The PANI ES showed the characteristic peaks at 1630, 1484, 1302, and 1145 cm<sup>-1</sup>, which were assigned to the nonsymmetric benzene ring stretching vibration, the stretching vibration of benzenoid ring, the C–H stretching vibration with aromatic conjugation and the N–Q–N (Q denotes quinoid ring) stretching mode,<sup>33</sup> respectively. Compared with the PANI ES, the PANI/P-PVA showed a strong absorbance peak at 1690 cm<sup>-1</sup> due to the overlap of the absorbance

frequency of the  $\text{—P—O—C—}$  groups of the P-PVA and the in-plane-bending vibration of the  $\text{C—H}$  of PANI. The obvious step up of the absorbance peak around  $3390\text{ cm}^{-1}$  was attributed to the  $\text{—OH}$  stretching. The results suggested that P-PVA molecules had been adsorbed and/or doped in the PANI particles.

XRD patterns of the PANI ES and PANI/P-PVA are shown in Figure 4. For the PANI ES, the crystalline peak at  $2\theta = 25^\circ$  was due to the periodicity perpendicular to polyaniline chain in its emeraldine salt form, indicating that PANI was partly crystalline.<sup>34</sup> Compared with the PANI ES, the similar crystalline peak at  $2\theta = 25^\circ$  could be obtained from the XRD pattern of the PANI/P-PVA. Meanwhile, the novel crystalline peak at  $2\theta = 20^\circ$  was due to the crystallization of phosphorylate ester side chain.<sup>35</sup> The results indicated that the PANI/P-PVA was partly crystalline in nature.

The electrical conductivity of the PANI ES powder was  $4.05\text{ S/cm}$  while that of the PANI/P-PVA powder was found to be  $7.26\text{ S/cm}$ , and the PANI content of the PANI/P-PVA is  $74.03\text{ wt } \%$ . The good electrical conductivity of the PANI/P-PVA could be attributed to the codoping of P-PVA and the partly crystalline structure of the PANI/P-PVA.

**Physical Properties of Coatings.** The excellent physical properties of coatings are a primary prerequisite for fulfilling the anticorrosion function of coatings system.<sup>19</sup> The mechanical properties of the coating samples were shown in Table 1. All the three PANI/P-PVA-containing coatings and the  $2.5\text{ wt } \%$  PANI ES had higher impact resistances than the epoxy film. The tensile strength test detected the good ductility of the coatings with PANI particles. It was found clearly that the PANI/P-PVA-containing coatings and the PANI ES-containing coating had lower pencil hardness and adhesion than the epoxy film, which indicated that the presence of PANI particles obviously influences the hardening of epoxy film and makes it less hard and more ductile and elastic, similar to what was observed by Kalendová et al.<sup>19</sup> Once PANI was introduced into epoxy, the

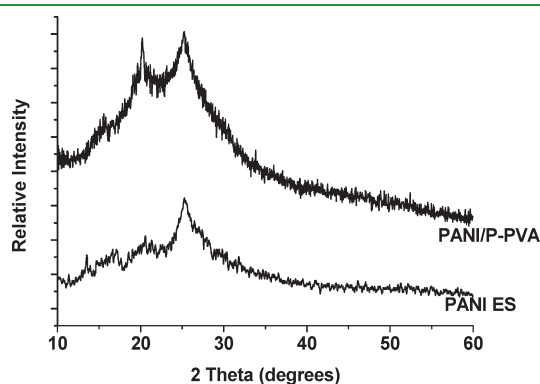


Figure 4. XRD patterns of PANI ES and PANI/P-PVA.

adhesion of the coatings suffered from a remarkable reduction. However, all the PANI/P-PVA-containing coatings showed better adhesion than the  $2.5\text{ wt } \%$  PANI ES, which is mainly attributed to the good dispersibility and presence of phosphates in PANI/P-PVA particles. Meanwhile the three PANI/P-PVA-containing coatings, especially the  $2.5\text{ wt } \%$  PANI/P-PVA, showed better overall mechanical properties than the  $2.5\text{ wt } \%$  PANI ES. The results suggested that the PANI/P-PVA particles had more positive effects on mechanical properties than the PANI ES particles may due to the optimum size, suitable shape and distribution of the PANI/P-PVA particles, and their good compatibility with the epoxy blinder.

The barrier effects of the PANI/P-PVA particles and PANI ES particles were also shown in Table 1. Compared to the  $2.5\text{ wt } \%$  PANI ES, the  $2.5\text{ wt } \%$  PANI/P-PVA showed about  $51.39\%$  and  $32.28\%$  reduction in  $\text{O}_2$  and  $\text{H}_2\text{O}$  permeability, respectively. In addition, both the  $1.0\text{ wt } \%$  PANI/P-PVA and  $4.0\text{ wt } \%$  PANI/P-PVA exhibited better barrier properties than the  $2.5\text{ wt } \%$  PANI ES. The low small-molecule permeability was mainly attributed to the good barrier properties of the PANI/P-PVA particles/nanolayers.<sup>32</sup>

**OCP Studies.** The variation in OCP with time for coated steels in  $3.0\text{ wt } \%$  NaCl is shown in Figure 5. The initial OCP values of the bare steel and the pure epoxy film-coated steel were  $-0.566\text{ V vs SCE}$  and  $-0.443\text{ V vs SCE}$ . After  $720\text{ h}$  exposure to  $3.0\text{ wt } \%$  NaCl solution, the OCP value of the pure epoxy film decreased to  $-0.643\text{ V vs SCE}$ . Initially, the OCP value of the  $2.5\text{ wt } \%$  PANI ES-coated steel was about  $-0.251\text{ V vs SCE}$  while that of the  $1.0\text{ wt } \%$  PANI/P-PVA,  $2.5\text{ wt } \%$  PANI/P-PVA, and  $4.0\text{ wt } \%$  PANI/P-PVA-coated steel was  $-0.230$ ,  $-0.177$ , and  $-0.189\text{ V vs SCE}$ , respectively. The OCP values of

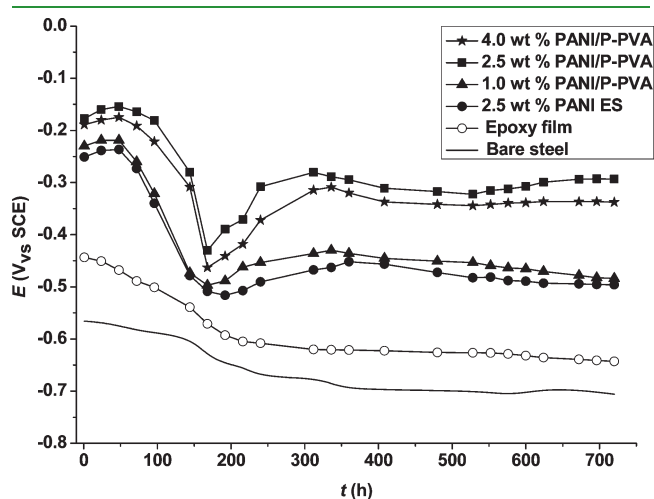


Figure 5. OCP variation of coated steels in  $3.0\text{ wt } \%$  NaCl.

Table 1. Mechanical Properties of the Coatings

samples	tensile strength (MPa)	impact resistance (cm)	pencil hardness	adhesion degree	permeability of $\text{O}_2$ (%)	permeability of $\text{H}_2\text{O}$ ( $\text{g}/(\text{m}^2\text{ h})$ )
epoxy film	18.9	35	H	4B	0.94	137.54
$1.0\text{ wt } \%$ PANI/P-PVA	19.4	45	B~HB	3B	0.81	113.82
$2.5\text{ wt } \%$ PANI/P-PVA	23.6	50	HB	3B	0.37	75.17
$4.0\text{ wt } \%$ PANI/P-PVA	25.2	45	HB	3B	0.31	65.37
$2.5\text{ wt } \%$ PANI ES	21.4	40	B~HB	2B	0.72	111.00

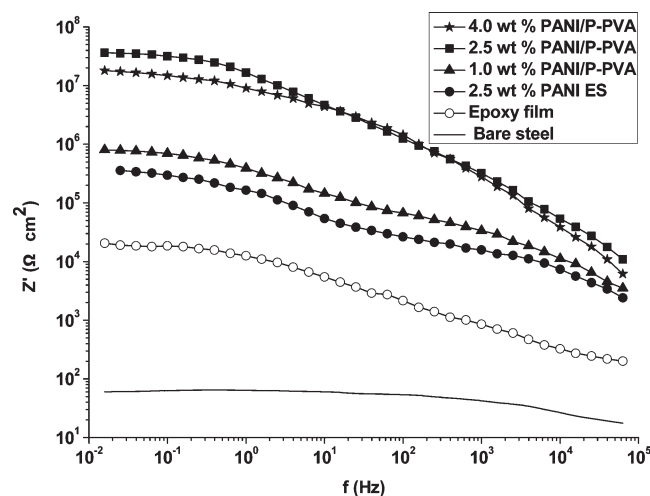


Figure 6. Impedance plots of the coated steels in 3.0 wt % NaCl after 50 days immersion.

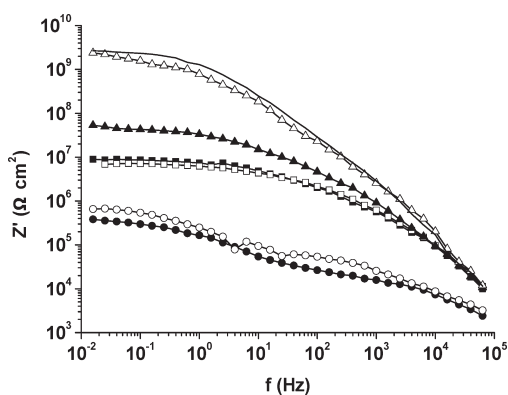


Figure 7. Impedance plots of 2.5 wt % PANI ES-coated steel in 3.0 wt % NaCl: —, initial;  $\Delta$ , 1 day;  $\blacktriangle$ , 4 days;  $\square$ , 7 days;  $\blacksquare$ , 14 days;  $\circ$ , 28 days;  $\bullet$ , 50 days.

all the samples containing PANI were decreased initially and shifted to noble direction after 168 h immersion, indicating that PANI in the coatings was able to passivate the iron surface in 3.0 wt % NaCl media. It also could be observed that the OCP shifted more noble with the higher PANI/P-PVA content and all the three PANI/P-PVA-containing coated steels exhibited higher OCP value than the 2.5 wt % PANI ES-coated steel. In fact, for 2.5 wt % PANI/P-PVA, the OCP remains at  $-0.293$  V vs SCE even after 720 h of exposure to saline atmosphere. Although the OCP value of the 2.5 wt % PANI ES-coated steel decreased to  $-0.496$  V vs SCE after 720 h. The results indicated that the coatings containing PANI/P-PVA were able to maintain more noble potential values in comparison to the coatings containing PANI ES during the whole immersion period. It indicated that PANI/P-PVA was able to passivate the steel better. Many earlier studies have shown that the OCP values of PANI-containing coated steel is higher than bare steel by  $100\sim 500$  mV in 3.0 wt % NaCl solution because of the passivation of iron.<sup>5,27</sup>

**EIS Studies of Coated Steel in 3.0 wt % NaCl.** EIS was used to investigate the protective nature of the coatings by measuring the coatings resistance ( $R_c$ ) and the coatings capacitance ( $C_c$ ) of

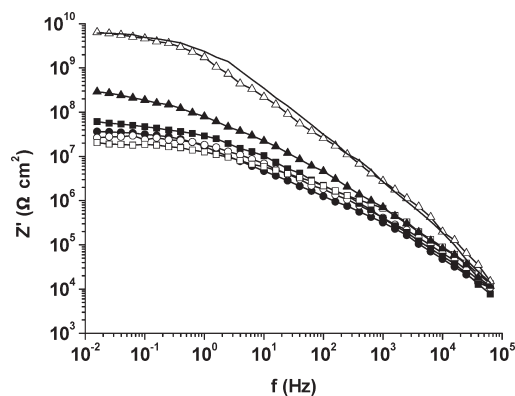


Figure 8. Impedance plots of 2.5 wt % PANI/P-PVA-coated steel in 3.0 wt % NaCl: —, initial;  $\Delta$ , 1 day;  $\blacktriangle$ , 4 days;  $\square$ , 7 days;  $\blacksquare$ , 14 days;  $\circ$ , 28 days;  $\bullet$ , 50 days.

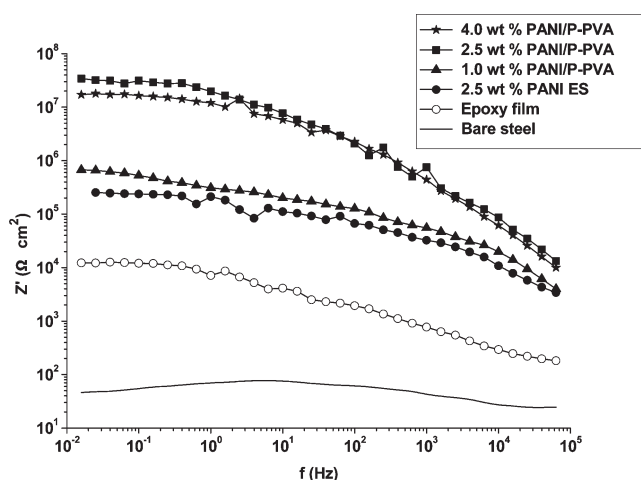
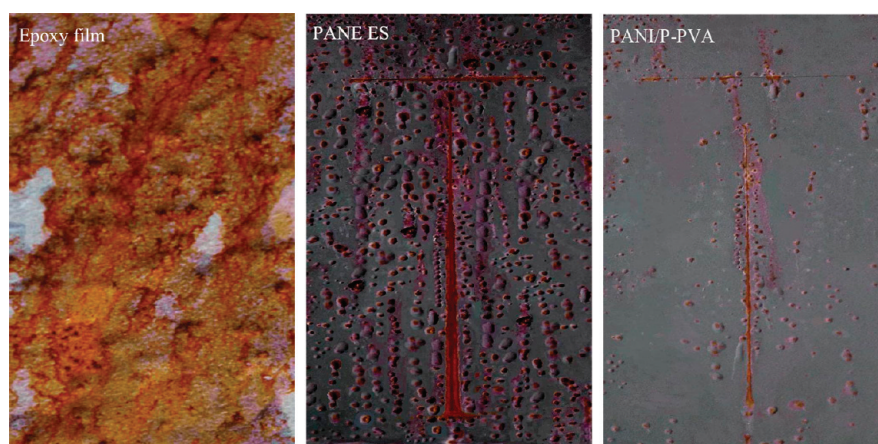


Figure 9. Impedance plots of the coated steels in 3.0 wt % NaCl after 30 days exposure to salt spray test.

the coatings. Coatings with high resistance values ( $>1 \times 10^7 \Omega \text{ cm}^2$ ) and low capacitance values ( $<1 \times 10^{-9} \text{ F cm}^{-2}$ ) have been found to offer corrosion protection of steel.<sup>28</sup>

Impedance plots (Bode plots, impedance versus frequency) of the bare steel, pure epoxy film-coated steel, 2.5 wt % PANI ES, 1.0 wt % PANI/P-PVA, 2.5 wt % PANI/P-PVA, and 4.0 wt % PANI/P-PVA-coated steels after 50 days of immersion in 3.0 wt % NaCl are shown in Figure 6. Obviously, 2.5 wt % PANI/P-PVA possessed the highest  $R_c$  value ( $3.5 \times 10^7 \Omega \text{ cm}^2$ ) at a low frequency of 0.025 Hz, followed by 4.0 wt % PANI/P-PVA ( $1.74 \times 10^7 \Omega \text{ cm}^2$ ), 1.0 wt % PANI/P-PVA ( $7.85 \times 10^6 \Omega \text{ cm}^2$ ), and 2.5 wt % PANI ES ( $3.58 \times 10^6 \Omega \text{ cm}^2$ ). Pure epoxy film-coated steel just had a low  $R_c$  value of  $1.87 \times 10^4 \Omega \text{ cm}^2$  because of the poor barrier property of epoxy film without any filler (Table 1). When the pure epoxy film-coated steel was immersed in 3.0 wt % NaCl, small molecules ( $\text{H}_2\text{O}$  and  $\text{O}_2$ ) or ions could easily penetrated epoxy film and freely corrode iron, resulting in a low resistance. Once PANI was introduced, coating resistance could be maintained at relatively high values, indicating the better corrosion protection of PANI-containing coatings than that of pure epoxy film. Conducting PANI exhibits a redox potential close to silver. It could ennoble iron surfaces of and form a thin





**Figure 10.** Photograph of pure epoxy-coated panel, 2.5 wt % PANI ES-coated panel, and 2.5 wt % PANI/P-PVA-coated panel after 30 days exposure to salt spray test.

but dense passive  $\text{Fe}_2\text{O}_3$  layer on iron surfaces. Hence PANI works as a noble metal and physical filler in PANI-containing coatings. Remarkably, all three PANI/P-PVA-containing coatings showed higher resistance values than PANI ES, suggesting PANI/P-PVA-containing coatings could provide more effective corrosion protection. It could be explained by the better physical properties of PANI/P-PVA-containing coatings (Table 1), such as good adhesion degree and low permeability of small molecules. PANI/P-PVA had an excellent dispersibility in waterborne epoxy matrix and could form PANI-containing coatings with dense and compact structure. Although the inadequate compatibility between PANI ES and waterborne epoxy matrix would wreck the mechanical property of PANI ES-containing coatings. At last, the increase of impedance values at high PANI/P-PVA contents various frequency regions could be interpreted as the barrier effect of PANI/P-PVA well-dispersed in epoxy matrix.<sup>26</sup>

For comparison, the specific impedance behavior of the 2.5 wt % PANI ES and 2.5 wt % PANI/P-PVA are shown in Figures 7 and 8. Initially, the 2.5 wt % PANI ES coatings had a  $R_c$  value of  $2.67 \times 10^9 \Omega \text{ cm}^2$  that decreased to  $6.90 \times 10^6 \Omega \text{ cm}^2$  after 7 days of immersion. Then, the  $R_c$  value exhibited a weak gain and increased to  $8.92 \times 10^6 \Omega \text{ cm}^2$  after 14 days of immersion. There was a sharp decrease in  $R_c$  value after 14 days, and it reached  $3.82 \times 10^5 \Omega \text{ cm}^2$  after 50 days of immersion. The  $R_c$  value of the 2.5 wt % PANI/P-PVA is found to decrease from  $6.20 \times 10^9 \Omega \text{ cm}^2$  to  $2.06 \times 10^7 \Omega \text{ cm}^2$  after 7 days of immersion. Afterward the  $R_c$  value increased to  $6.09 \times 10^7 \Omega \text{ cm}^2$  after 14 days of immersion and reached to  $3.64 \times 10^7 \Omega \text{ cm}^2$  after 50 days of immersion. For both coatings, the increased resistance values after an initial decrease could be due to the passivation effect of PANI. PANI behaves like a noble metal since its redox potential is close to silver due to its conducting nature. Hence it ennobles the surface of metals and forms a thin but dense passive  $\text{Fe}_2\text{O}_3$  layer on the surface. During the initial exposure period, the diffusion of water as well as other ions into the coating resulted in the decreasing in coatings resistance at low frequency. With increasing exposure time, mild steel suffered from corrosion, accompanied by a reduction of PANI-Emeraldine salt (PANI-ES) to PANI-Leucosalt (PANI-LS). The reduction is benefit to the oxidation of Fe to  $\text{Fe}^{2+}$  or  $\text{Fe}^{3+}$ . Then PANI-LS could be reoxidized to PANI-ES in corrosive environment. The redox

property of PANI could contribute to the formation of  $\text{Fe}_2\text{O}_3$  layer on iron surface, which lead to the increasing in resistance at low frequency. After a long exposure time, the coatings resistance decreased at low frequency due to the corrosion rate is higher than the passivation rate of iron. Additionally, the  $C_c$  values of the 2.5 wt % PANI ES decreased from  $8.02 \times 10^{-10} \text{ F cm}^{-2}$  to  $8.92 \times 10^{-4} \text{ F cm}^{-2}$  after 50 days of immersion, which indicated that water uptake of the PANI ES-containing coatings was increased obviously due to the poor dispersibility of PANI ES and the weak compatibility of the PANI ES/waterborne matrix system. Compared with the 2.5 wt % PANI ES, the 2.5 wt % PANI/P-PVA could remain its  $C_c$  values at  $0.51 \sim 4.01 \times 10^{-9} \text{ F cm}^{-2}$  during the entire immersion period because of the low permeation of water through the coatings, implying that the better dispersibility of the PANI/P-PVA in waterborne matrix than that of PANI ES. The results showed that the 2.5 wt % PANI/P-PVA was able to offer protection up to 50 days and more protective than 2.5 wt % PANI ES in 3.0 wt % NaCl solution due to redox catalytic property of PANI and barrier effect of PANI/P-PVA nanoparticles dispersing well in epoxy matrix. Earlier studies<sup>10,12</sup> have shown that the corrosion protection ability of the coatings on steel is found to be high if the resistance value of the coatings is greater than  $1 \times 10^7 \Omega \text{ cm}^2$ . Sathiyarayanan have shown from their studies that solvent-based epoxy coatings containing 1.0 wt % PANI is able to protect steel in 3.0 wt % NaCl solution effectively.<sup>27</sup> In their studies, the resistance value of the 2.5 wt % PANI/P-PVA could reach  $9.39 \times 10^8 \Omega \text{ cm}^2$  after 50 days of exposure to 3.0 wt % NaCl.

**EIS Studies of Coated Steel after Salt Spray Exposure Test.** Impedance plots of the bare steel, pure epoxy film-coated steel, 2.5 wt % PANI ES, 1.0 wt % PANI/P-PVA, 2.5 wt % PANI/P-PVA, and 4.0 wt % PANI/P-PVA-coated steels after 30 days of salt spray exposure are shown in Figure 9. It can be seen that the 2.5 wt % PANI/P-PVA and 4.0 wt % PANI/P-PVA had much higher resistance than the 2.5 wt % PANI ES, especially at low frequency, which is associated with ionic transport through the film.

The appearance of pure epoxy-coated panel, 2.5 wt % PANI ES-coated panel and 2.5 wt % PANI/P-PVA-coated panel after salt spray test for 30 days is shown in Figure 10. It could also be seen that the pure epoxy-coated panel suffered from aggravating corrosion in large-scale with red rust ( $\text{Fe}_3\text{O}_4$ ) layers. For

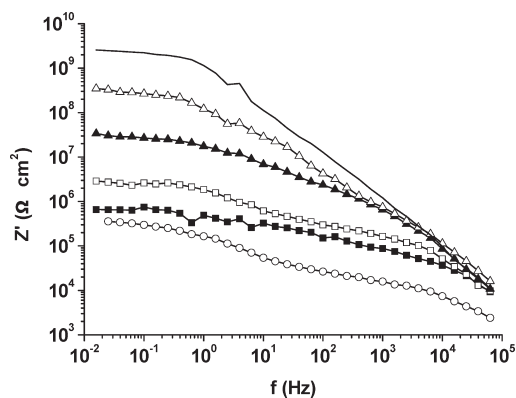


**Figure 11.** Impedance plots of 2.5 wt % PANI ES-coated steel in 3.0 wt % NaCl after salt spray exposure: —, initial; Δ, 1 day; ▲, 4 days; □, 7 days; ■, 14 days; ○, 30 days.

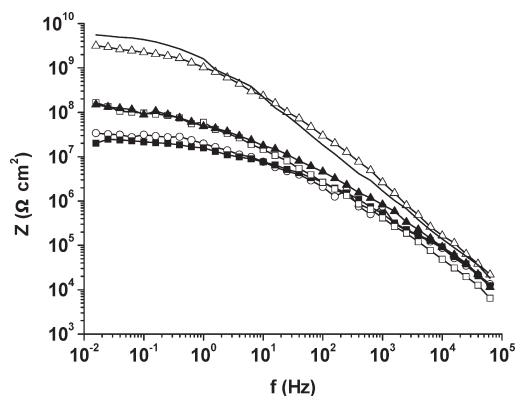


**Figure 12.** Impedance plots of 2.5 wt % PANI/P-PVA-coated steel in 3.0 wt % NaCl after salt spray exposure: —, initial; Δ, 1 day; ▲, 4 days; □, 7 days; ■, 14 days; ○, 30 days.

the 2.5 wt % PANI ES, coatings on the steel panel bubbled severely and obvious corrosion was found, whereas localized corrosion was observed for the 2.5 wt % PANI/P-PVA and a slight rust formation was found in the scribed areas of the 2.5 wt % PANI/P-PVA.

The impedance behavior of 2.5 wt % PANI ES and 2.5 wt % PANI/P-PVA after salt spray test is shown in Figures 11 and 12. The variation of the  $R_c$  and the  $C_c$  values with time are also obtained. In the case of the 2.5 wt % PANI ES, it was found that the initial  $R_c$  value was  $2.57 \times 10^9 \Omega \text{ cm}^2$ , which decreased to  $2.89 \times 10^6 \Omega \text{ cm}^2$  after 7 days salt spray exposure and continued to decrease to  $3.58 \times 10^5 \Omega \text{ cm}^2$  after 30 days salt spray exposure in 3.0 wt % NaCl. However, in the case of 2.5 wt % PANI/P-PVA, the  $R_c$  values remained higher than  $3.40 \times 10^7 \Omega \text{ cm}^2$  even after 30 days salt spray exposure in 3.0 wt % NaCl. These results indicated that the 2.5 wt % PANI/P-PVA was highly protective in comparison with the 2.5 wt % PANI ES, because the  $R_c$  value after 30 days salt spray exposure was found to be about 100 times higher for the 2.5 wt % PANI/P-PVA. This result was similar to what was observed by Chang<sup>30</sup> under the PANI dispersion coatings on steel. They found that the corrosion protection of PANI-clay nanocomposites prepared from in situ emulsion polymerization should be resulted from both the redox catalytic property of PANI and barrier effect of clay platelets dispersing in composites. Therefore, in this study, the high

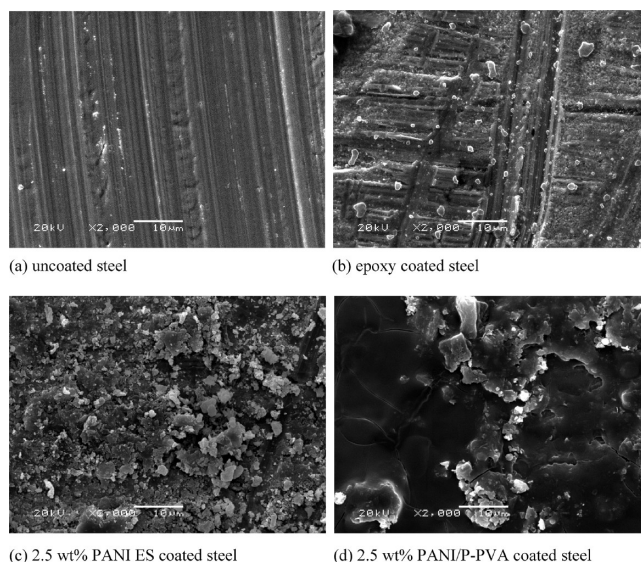


**Figure 13.** SEM images of the interface between steel and coatings.

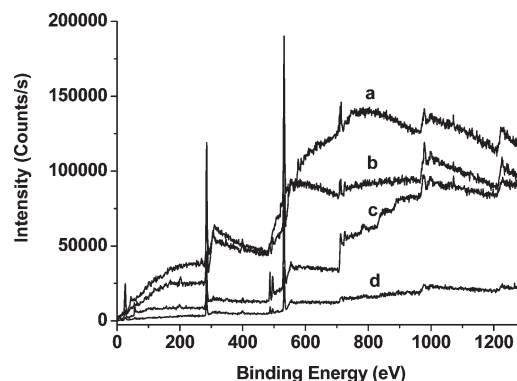


**Figure 14.** XPS spectra of the interface between steel and coatings: (a) uncoated steel; (b) epoxy-coated steel; (c) 2.5 wt % PANI ES-coated steel; and (d) 2.5 wt % PANI/P-PVA-coated steel.

$R_c$  values of the PANI/P-PVA-containing coatings in various frequency regions could also be attributed to the formation of passive layer and barrier effect of the well dispersed PANI/P-PVA nanoparticles.

**Surface Characterization.** The morphology of the interfaces between treated steels and coatings is shown in Figure 13. It can be seen that the sand blasted mild steel exhibited obvious scratch, caused by rubbing the surface with sandpaper (Figure 13a). It is clear that the interface between pure epoxy and mild steel showed difference from that of uncoated mild steel after 50 days exposure to 3.0 wt % NaCl. There was a thin layer with some particles on the interface, which could be attributed to the interaction between epoxy and steel substrate and rust  $\text{Fe}_3\text{O}_4$  (Figure 13b). In the presence of 2.5 wt % PANI ES (Figure 13c), tough lamellae are observed on a thin layer at the surface. For PANI/P-PVA-coated steel (Figure 13d), a denser and more compact layer formed on the metal surface, which was avial to improving the corrosion resistance of the material.

XPS analysis of the interfaces between the coatings and steel substrates was carried and the results were given in Figure 14 and Table 2. For the untreated steel, C 1s, O 1s, N 1s, and Fe 2p



Table 2. XPS Analyses of Steel Surfaces (at %)

samples	C 1s	O 1s	N 1s	Fe 2p	Cl 1s	Na 1s	P 2p
uncoated mild steel	26.14	37.42	1.81	34.63			
pure epoxy	50.06	34.78	0.52	10.06	2.51	1.07	
2.5% PANI ES	56.68	36.15	2.42	4.76	1.59	0.76	
2.5% PANI/P-PVA	55.84	36.64	2.81	3.63	0.73	0.63	0.95

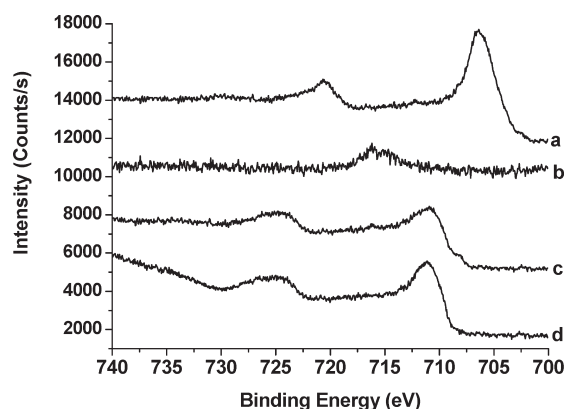


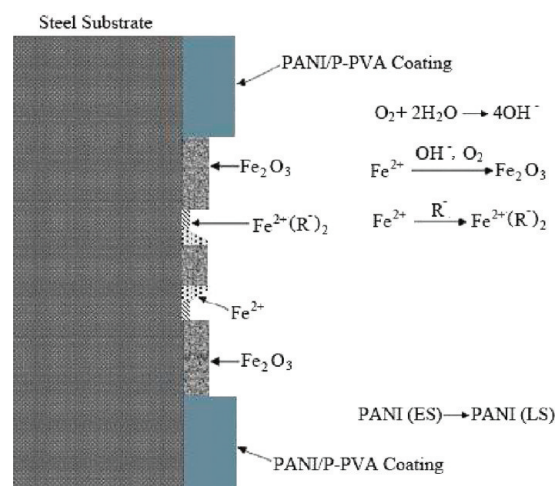
**Figure 15.** XPS Fe 2p spectra of: (a) uncoated steel; (b) epoxy-coated steel; (c) 2.5 wt % PANI ES-coated steel; and (d) 2.5 wt % PANI/P-PVA-coated steel.

signals are detected. Once introducing epoxy, Fe 2p content was decreased from 34.63 at % to 10.06 at %, mainly because of the interaction between epoxy and steel substrate, which was consistent with the SEM result (thin epoxy/steel layer). The present of Cl and Na elements was attributed to the permeation of ions from 3.0 wt % NaCl. For 2.5 wt % PANI ES-coated steel, N 1s content was significantly higher than that on the interface of epoxy-coated steel, whereas Cl 1s and Na 1s contents decreased. The increasing N 1s content proved the presence of PANI on the interface. The low Cl 1s and Na 1s contents demonstrated that 2.5 wt % PANI ES-containing coatings possessed a higher barrier property than pure epoxy film. Among all the samples, 2.5 wt % PANI/P-PVA-coated steel showed the highest N 1s content and lowest Cl 1s and Na 1s contents accompanied by the existence of P 2p. The result indicated that the interaction of PANI/P-PVA/steel substrates was energetic. And the existence of P 2p would promote the formation of a compact PANI/P-PVA/iron layer.

Figure 15 presents XPS spectra for Fe 2p for each of the four samples. For the untreated steel, the peak at about 706.7 eV showed that iron was partially in metallic state. While XPS spectra of the pure epoxy-coated steel showed a single at about 716.4 eV indicated that the iron on interface was mainly in divalent state, such as FeO, and Fe<sub>3</sub>O<sub>4</sub>. For 2.5 wt % PANI ES-coated steel, the obvious peak at about 710.7 eV indicated that the iron on interface mainly was composed of Fe<sub>2</sub>O<sub>3</sub> and Fe<sub>3</sub>O<sub>4</sub>.<sup>35</sup> The typical peak at 710.9 eV of 2.5 wt % PANI/P-PVA-coated steel showed that iron mainly existed as Fe<sub>2</sub>O<sub>3</sub> on the interface. Combining with both SEM and XPS results, we conclude that PANI/P-PVA have strong interaction with steel and a compact passive Fe<sub>2</sub>O<sub>3</sub> layer could be formed on the interface between PANI/P-PVA-containing coatings and steel substrate.

**Proposed Mechanism of Corrosion Protection.** The corrosion protection of the PANI-containing coatings on steel is mainly

Scheme 2. Proposed Mechanism of Iron Passivation by PANI/P-PVA-Coated Steel



brought about by three factors: formation of a passivation layer, barrier effects which prevent oxygen and moisture from reaching the metal substrate, and adhesion. In their study, phosphate anions could form the insoluble compounds FeHPO<sub>4</sub> and Fe<sub>3</sub>(PO<sub>4</sub>)<sub>2</sub> with the iron atoms present in steel, resulting in a passive film. In the case of the PANI/P-PVA containing coatings, the passivation effect was offered not only by the formation of Fe<sub>2</sub>O<sub>3</sub> layer but also by the formation of iron–phosphate secondary complex<sup>36,37</sup> because of the redox reaction of the PANI/P-PVA. The proposed mechanism of passivation of steel by the PANI/P-PVA is schematically shown in Scheme 2. During the immersion in 3.0% NaCl solution, an oxidation of Fe to Fe<sup>2+</sup> or Fe<sup>3+</sup> takes place through the passive oxide film. The oxidation is accompanied by the reduction of PANI-ES to PANI-LS with forming a passive Fe<sub>2</sub>O<sub>3</sub> layer.<sup>38</sup> To maintain the neutrality in coatings, the reduction of PANI is further accompanied by releasing the anionic phosphoric dopant (R<sup>−</sup>). These phosphate ions helped to produce the insoluble Fe<sup>2+</sup>(R<sup>−</sup>)<sub>2</sub> and form passive film on iron at the defect. Because of these passive layers, PANI/P-PVA-containing coatings was able to offer higher corrosion protection, which be evidenced by the OCP results (Figure 6). But in the case of PANI ES-containing coatings, there was no phosphate ion to form an iron–phosphate secondary complex.

For the PANI/P-PVA-containing coatings system, the barrier properties were improved no doubt due to the excellent dispersibility of the colloidal PANI/P-PVA nanoparticles. The small and uniform dispersion of PANI with nano size would decrease the permeability to small molecules (e.g., H<sub>2</sub>O and O<sub>2</sub>) and increase the efficiency of corrosion inhibition.<sup>39</sup> The good barrier properties of PANI/P-PVA-containing coatings also could be evidenced by its high resistances (Figure 8 and Figure 12) after exposure to immersion tests and salt spray tests, and the low small-molecule permeability (Table 1). For the PANI ES-containing coating system, the macroscopic particles of PANI with poor dispersibility and their high volume fraction were likely to wreck the mechanical property of coatings and increased the permeability to small molecules.<sup>40</sup> In addition, PANI ES had an inferior compatibility with the waterborne epoxy matrix because of its insoluble nature and poor dispersibility in aqueous media, resulting in a bad adhesion between PANI ES-containing coatings and steel. The bad adhesion could be evidenced by PANI

ES-containing coatings with large area of bubbling and pitting (Figure 10). On the contrary, PANI/P-PVA-containing coating system had a satisfactory compatibility because of the excellent dispersibility of the colloidal PANI/P-PVA nanoparticles, which was beneficial to improving the adhesion (Table 1). Moreover, the present of phosphates in the PANI/P-PVA coatings was a positive factor for improving adhesion to steel. The high adhesion was consequentially available to promoting the anticorrosive performance of PANI/P-PVA-containing coatings on steel.

## CONCLUSION

Conducting PANI/P-PVA nanoparticles was synthesized by the chemical oxidative polymerization of aniline in presence of the P-PVA. The results indicated that the PANI/P-PVA nanoparticles exhibited significant dispersibility in aqueous media. The waterborne PANI/P-PVA-containing coatings was prepared and applied on mild steel by a dipping method. The corrosion protection property of the coatings on mild steel exposed to 3.0 wt % NaCl solution was investigated by measurements of the OCP versus time of exposure and EIS. The variations in the OCP values and EIS spectra with time of exposure demonstrated that the waterborne PANI/P-PVA-containing coatings with the PANI/P-PVA of 2.5 wt % was able to offer higher corrosion protection than the PANI ES-containing coatings with PANI ES content of 2.5 wt % because of the effective  $\text{Fe}_2\text{O}_3$  passive layer and uniform distribution of the system. And the formation of the  $\text{Fe}_2\text{O}_3$  passive layer was evidenced by SEM and XPS analysis.

## AUTHOR INFORMATION

### Corresponding Author

\*Fax: +86 931 8912582. E-mail: pliu@lzu.edu.cn.

## REFERENCES

- Bhadra, S.; Khastgir, D.; Singha, N. K.; Lee, J. H. *Prog. Polym. Sci.* **2009**, *34*, 783–810.
- Xiong, S.; Wei, J.; Jia, P.; Yang, L.; Ma, Jan.; Lu, X. *ACS Appl. Mater. Interfaces* **2011**, *3*, 782–788.
- Mengoli, G.; Munari, M. T.; Bianco, P.; Musiani, M. M. *J. Appl. Polym. Sci.* **1981**, *26*, 4247–4257.
- DeBerry, D. W. *J. Electrochem. Soc.* **1985**, *132*, 1022–1026.
- Meroufel, A.; Deslouis, C.; Touzain, S. *Electrochim. Acta* **2008**, *53*, 2331–2338.
- Plesu, N.; Ilia, G.; Pascariu, A.; Vlase, G. *Synth. Met.* **2006**, *156*, 230–238.
- Kamaraj, K.; Sathiyarayanan, S.; Muthukrishnan, S.; Venkatachari, G. *Prog. Org. Coat.* **2009**, *64*, 460–465.
- Williams, G.; McMurray, H. N. *Electrochim. Acta* **2009**, *54*, 4245–4252.
- Fang, J.; Xu, K.; Zhu, L.; Zhou, Z.; Tang, H. *Corros. Sci.* **2007**, *49*, 4232–4242.
- Spinks, G. M.; Dominis, A. J.; Wallace, G. G.; Tallman, D. E. *J. Solid State Electrochem.* **2002**, *6*, 85–100.
- Adhikari, A.; Claesson, P.; Pan, J.; Leygraf, C.; Deidinaite, A.; Blomberg, E. *Electrochim. Acta* **2008**, *53*, 4239–4247.
- Wessling, B.; Posdofer, J. *Electrochim. Acta* **1999**, *44*, 2139–2147.
- Wessling, B. *Synth. Met.* **1997**, *85*, 1313–1318.
- Beard, B. C.; Spellane, P. *Chem. Mater.* **1997**, *9*, 1949–1953.
- Kinlen, P. J.; Silverman, D. C.; Jeffreys, C. R. *Synth. Met.* **1997**, *85*, 1327–1332.
- Torresi, R. M.; Souza, S.; Pereira da Silva, J. E.; Cordoba de Torresi, S. I. *Electrochim. Acta* **2005**, *50*, 2213–2218.
- Lai, M.; Chang, K.; Yeh, J.; Liou, S.; Hsieh, M.; Chang, H. *Eur. Polym. J.* **2007**, *43*, 4219–4228.
- Chen, F.; Ye, F. Y.; Chu, G. C.; Guo, J. S.; Huo, L. X. *Prog. Org. Coat.* **2010**, *67*, 60–65.
- Kalendova, A.; Sapurina, I.; Stejskal, J.; Vesely, D. *Corros. Sci.* **2008**, *50*, 3549–3560.
- Jafarzadeh, S.; Thormann, E.; Rönneval, T.; Adhikari, A.; Sundell, P. E.; Pan, J.; Claesson, P. M. *ACS Appl. Mater. Interfaces* **2011**, *3*, 1681–1691.
- Koo, C. M.; Jeon, B. H.; Chung, I. J. *J. Colloid Interface Sci.* **2000**, *227*, 316–321.
- Rhim, J. W.; Park, H. B.; Lee, C. S.; Jun, J. H.; Kim, D. S.; Lee, Y. M. *J. Membr. Sci.* **2004**, *238*, 143–151.
- Suzuki, M.; Yoshida, T.; Koyama, T.; Kobayashi, S.; Kimura, M.; Hanabusa, K.; Shirai, H. *Polymer* **2000**, *41*, 4531–4536.
- Simoes, A. M.; Torres, J.; Picciochi, R.; Fernandes, J. *Electrochim. Acta* **2009**, *54*, 3857–3865.
- Samui, A. B.; Phadnis, S. M. *Prog. Org. Coat.* **2005**, *54*, 263–267.
- Moraes, S. R.; Vilca, D. H.; Motheo, A. J. *Eur. Polym. J.* **2004**, *40*, 2033–2041.
- Sathiyarayanan, S.; Muthukrishnan, S.; Venkatachari, G. *Electrochim. Acta* **2006**, *51*, 6313–6319.
- Chen, F.; Liu, P. *AIChE J.* **2011**, *57*, 599–605.
- Gimenez, V.; Reina, J. A.; Mantecon, A.; Cadiz, V. *Polymer* **1999**, *40*, 2759–2767.
- Chang, K. C.; Lai, M. C.; Peng, C. W.; Chen, Y. T.; Yeh, J. M.; Lin, C. L.; Yang, J. C. *Electrochim. Acta* **2006**, *51*, 645–653.
- Yeh, J. M.; Liou, S. J.; Lai, C. Y.; Wu, P. C.; Tsai, T. Y. *Chem. Mater.* **2001**, *31*, 1131–1134.
- Hsu, C. H.; Mansfeld, F. *Corrosion* **2001**, *57*, 747–748.
- Zhang, Z.; Wei, Y.; Wan, M. *Macromolecules* **2002**, *35*, 5937–5942.
- Zhang, Z.; Wan, M.; Wei, Y. *Adv. Funct. Mater.* **2006**, *16*, 1100–1104.
- Schauer, T.; Joos, A.; Dulog, L.; Eisenbach, C. D. *Prog. Org. Coat.* **1998**, *33*, 20–27.
- Moraes, S. R.; Huerta-Vilca, D.; Motheo, A. J. *Prog. Org. Coat.* **2003**, *48*, 28–33.
- Sedenkova, I.; Prokes, J.; Trochova, M. *Polym. Degrad. Stab.* **2007**, *93*, 428–435.
- Wei, Y.; Wang, J.; Jia, X.; Yeh, J. M.; Spellane, P. *Polymer* **1995**, *36*, 4535–4537.
- Stejskal, J. *J. Polym. Mater.* **2001**, *18*, 225–258.
- Talo, A.; Forsen, O.; Ylasaari, S. *Synth. Met.* **1999**, *102*, 1394–1395.